Computation and Simulation in Mechanical Sciences (CSMech)

Perfect position and oscillation frequency of nanosectors orbiting inside carbon nanotori

M. Hosseinzadeh, F. Sadeghi, R. Ansari

ORIGINAL PAPER

Open Access

Volume: 01

Issue: 01

Winter 2018

Page: 42-52

ISSN:

eISSN:

www.csmech.iaubanz.ac.ir

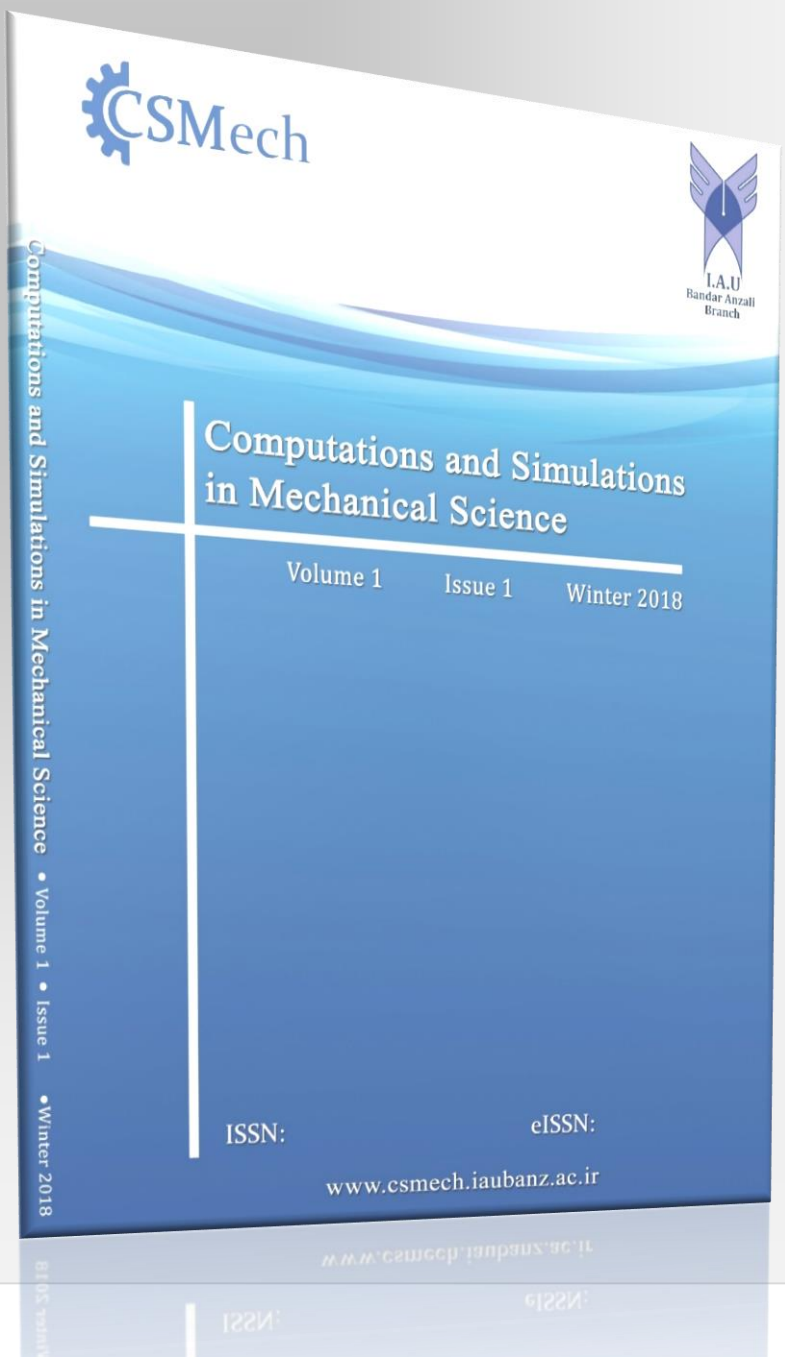

CSMech. **01**(01), 42-52, (2018)

Computations and Simulations in Mechanical Science

ORIGINAL PAPER

CSMech

www.csmech.iaubanz.ac.ir

Perfect position and oscillation frequency of nanosectors orbiting inside carbon nanotori

M. Hosseinzadeh[a], F. Sadeghi[b], R. Ansari[c,*]

[a] *Department of Mechanical Engineering, Mooj Institute of Technology and Higher Education, Bandar-e Anzali, Iran*

[b] *Young Researchers and Elite Club, Lahijan Branch, Islamic Azad University, Lahijan, Iran*

[c] *Department of Mechanical Engineering, University of Guilan, P.O. Box 3756, Rasht, Iran*

Abstract

This paper aims to develop a new semi-analytical method based on the continuum approximation and Lennard-Jones (LJ) potential function to investigate the potential energy and van der Waals (vdW) interaction force between sectors of nanotorus and carbon nanotori molecule. Following the present method, a semi-analytical formulation is achieved in terms of double integrals which can be readily employed to obtain the interactions. A semi-analytical expression is also presented to determine the oscillation frequency. The sector is assumed to be orbiting inside the carbon nanotori and is free to choose its perfect position inside this nanostructure. The effects of geometrical parameters such as tube and ring radii of nanotori as well as angle of nanosector on the variation of potential energy, vdW interaction force and frequency are examined. As a significant finding, it is shown that the oscillation frequency, which is in the gigahertz (GHz) range, is independent of the sector angle. Results of this study are shown to be consistent with the existing data and can be beneficial for the future studies on the GHz oscillators.

Article history

Received: 2017-12-21
Revised: 2018-02-07
Accepted: 2018-02-25

Keywords

Nanosector
Carbon nanotori
Lennard-Jones potential
Interaction force
Gigahertz oscillators

1. Introduction

The first sign of carbon nanotubes (CNTs) existence was reported by Iijima's paper in 1991 [1]. These nanostructures due to their outstanding thermal, mechanical and electrical properties have attracted much attention for applications in many nanoscale devices. Owing to the difficulties encountered for micromechanical oscillators to achieve frequencies up to gigahertz (GHz) range, it seemed worthwhile to seek alternative mechanisms to overcome this obstacle. Among these mechanisms, nanoscale oscillators or the so-called GHz oscillators are found to be appropriate candidates and have received much attention in recent years. Ultrafast optical filters and ultrasensitive nanoantennae are examples of the potential applications of such oscillators [2-4]. Numerous studies have been conducted so far concerning the mechanisms of different GHz oscillators such as CNT-CNT bundle [5], CNT- carbon nanoscroll [6] and C_{60}- CNT [7]. The concept of nanoscale oscillators was first initiated by Cumings and Zettl [8] through an experiment performed on two nested multi-walled carbon nanotubes (MWCNTs). In their study, an extruded inner core was released, which was later pulled back inside the outer tube due to the restoring van der Waals (vdW) interaction force generated from the outer tubes. Zheng and Jiang [9] using a continuum approximation of the discrete atoms, theoretically attained the frequency of these oscillators in the GHz range. Zheng et al. [10] by incorporating the effects of frictional forces into their proposed model proved that the influences of these forces on the oscillation frequency can be neglected. Legoas et al. [11, 12] studied the stability of such systems through the use of molecular dynamics (MD) simulations and confirmed the GHz frequency of these oscillators. Moreover, their investigations proved that the dynamic stability of these oscillators is possible when the diameter difference between the inner and the outer layers is about 3.4 Å. In spite of numerous studies conducted on the nanostructures using the MD simulations, this technique can pose some difficulties. The MD

*Corresponding author: R. Ansari
E-mail address: r_ansari@guilan.ac.ir

simulations are very time-consuming, especially when the number of involving atoms increases. Additionally, these simulations are only capable of solving the problem numerically, while the expressions derived within the continuum approximation can be in analytical or semi-analytical forms [13-16]. The continuum approximation due to its proven reliability and accuracy has been of especial interest to research workers. For instance, Hodak and Girifalco [17] evaluated the vdW interaction energies between CNTs and internal fullerenes with spherical and ellipsoidal shape and the interaction energy between walls of multi-walled nanotubes using the continuum approximation. Ansari et al. [18-23] used this method to analyze the oscillation frequency and distribution of vdW interactions between different nanostructures.

The aim of above studies was mainly concentrated to identify different characteristics of carbon nanostructures. In the following, another variety of carbon nanostructures, namely carbon nanotorus will be introduced. Carbon nanotorus formed from bending a CNT into a torus was discovered theoretically by Dunlap [24]. For more details concerning the other possible ways of forming a nanotorus, the reader is referred to [25-32]. Due to matchless geometry of carbon nanotorus, it captures exceptional physical properties including a higher reversible tension up to 39% [33] in comparison with that of CNTs which is about 5% [34, 35] and magnetic response which causes it to be appropriate as a system to study the quantum effects [36]. Bohua [37] studied the deformation, vibration, and buckling characteristics of a nanotorus embedded in an elastic medium and suggested a continuum model which provides a closed-form solution for the above-mentioned characteristics. Furthermore, Hilder and Hill [38] through the use of continuum approximation investigated the oscillatory behavior of an atom and a C_{60} fullerene orbiting inside a carbon nanotorus. Their study indicated that the equilibrium position of the atom and fullerene depends on the tube radius. Moreover, they exhibited that the orbiting body tends to move closer to the wall of the tube as the radius of the tube increases. The mechanics of a nanotorus oscillating along a carbon nanotube [39] and a nanosector orbiting concentrically inside a nanotorus [40] were also studied in the literature. Sabzyan and Kowsar [41] applied GHz rotating electric fields of various strengths and frequencies on a carbon nanotorus filled with water molecules by MD simulation. In another study [42], these researchers investigated the cyclotron motion of ions in a carbon nanotorus induced by GHz rotating electric field using MD simulations. A concise formalism to characterize nanometer-sized tori on the basis of CNTs was introduced by Chuang et al. [43]. In their study, stability of these structures was determined by combining ab initio density functional calculations with a continuum elasticity theory approach. Lee and Hill [44] investigated the mechanics of a nano logic gate, comprising a metallofullerene which is located inside a square-shaped single-walled carbon nanotorus comprising non-metallic, single-walled CNTs with perfect nanotoroidal corners. Glukhova et al. [45] proposed an experimental technique for increasing the yield of CNT nanotori utilizing the modified arc synthesis method. Farahani and Gao [46] studied the topological indices of nanotubes and nanotori. Loyola et al. [47] studied symmetry and color symmetry properties of Kepler, Heesch and Laves tilings embedded on a flat torus and their geometric realizations as tilings on a round torus in Euclidean 3-space.

This study investigates the mechanics of an offset nanosector orbiting inside a carbon nanotori molecule. The formulations of vdW interactions are given in terms of double integrals using the continuum approximation along with the 6-12 Lennard-Jones (LJ) potential function. Moreover, based on the Newton's second law and neglecting the gravitational and frictional forces, a simple semi-analytical expression is presented to evaluate the oscillation frequency. Finally, the influences of geometrical parameters on the minimum potential energy, vdW interaction force and oscillation frequency are examined.

2. Potential energy and interaction force

In order to determine the vdW interactions, the classical LJ potential function is applied here. The LJ potential between two atoms at a distance ρ apart is expressed by

$$\Phi(\rho) = -\frac{A}{\rho^6} + \frac{B}{\rho^{12}} \tag{1}$$

in which A and B denote the attractive and

repulsive constants, respectively. The total potential energy is obtained by summing the interaction energy for each atom pair as follows

$$E_{vdW} = \sum_i \sum_j \Phi(\rho_{ij}) \quad (2)$$

where $\Phi(\rho_{ij})$ represents the potential energy function for atoms i and j which are located at a distance ρ_{ij}. Using the continuum approximation which assumes that carbon atoms are uniformly distributed over the surfaces of the molecules, the double summation in Eq. (2) can be replaced by a double integral as

$$E_{vdW} = \eta_1 \eta_2 \int_{S_2} \int_{S_1} \Phi(\rho) dS_1 dS_2 \quad (3)$$

In the prior equation, η_1 and η_2 indicate the mean atomic surface densities of carbon atoms on each molecule and ρ denotes the distance between two typical surface elements dS_1 and dS_2.

Moreover, so as to obtain the vdW interaction force, one can differentiate the potential energy as

$$F_{vdW} = -\nabla E_{vdW} \quad (4)$$

3. Force balance for orbiting motion

In this section, the force balance for an offset nanosector orbiting inside a nanotori is briefly presented. As shown in Fig. 1, ε symbolizes the eccentricity distance between the centers of cross-sections of nanosector and perfect torus, in which nanosector is a sector of a perfect torus with the tube radius a.

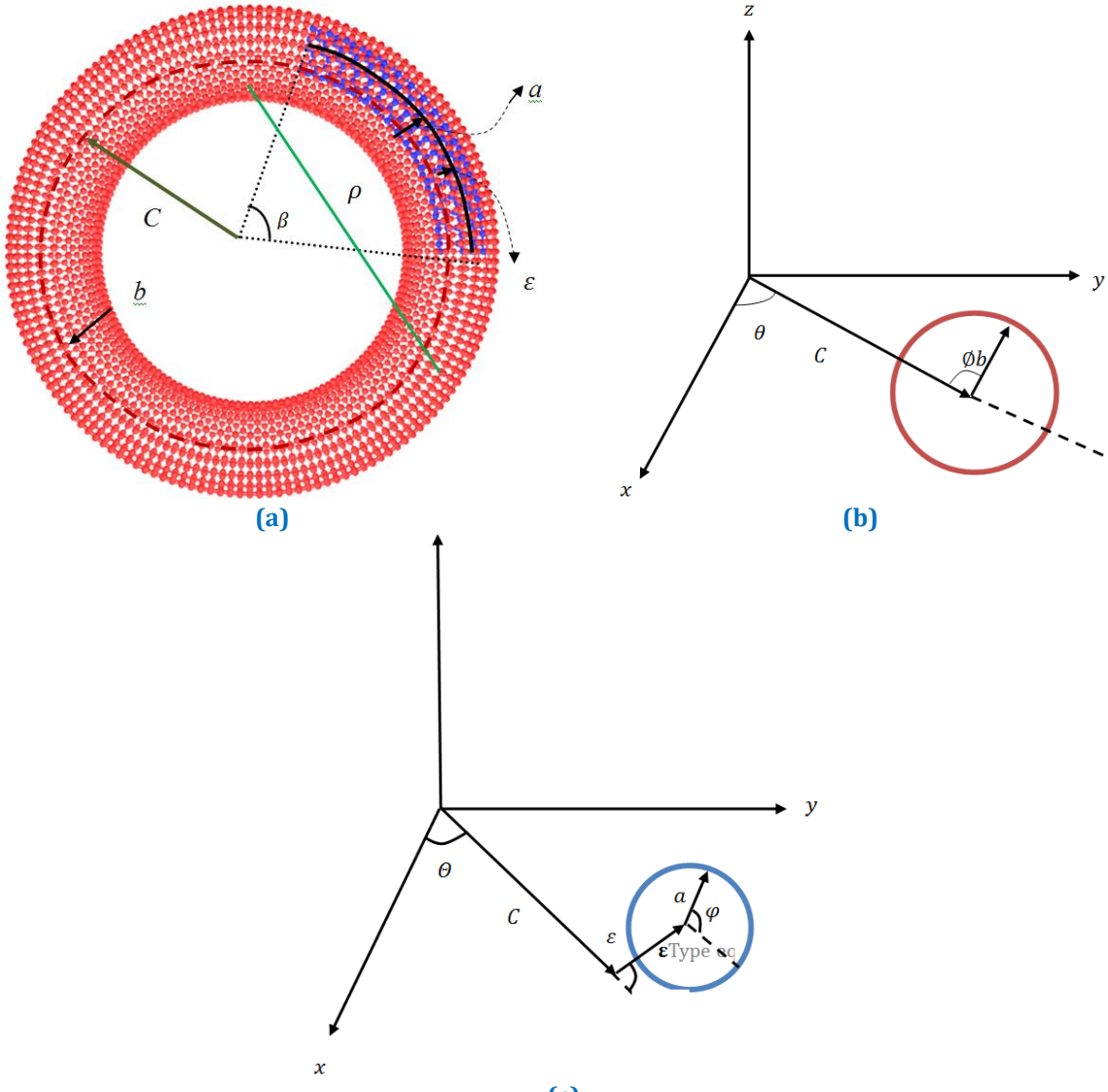

Fig. 1. Geometry of the considered mechanism **(a)** three-dimensional sketch of the nanosector inside a nanotori **(b)** cross-section of the nanotorus in its coordinate **(c)** cross-section of the nanosector in its coordinate

The tube radius and ring radius of the nanotori are also denoted by b and c, respectively. The rotating body experiences three forces while turning around the nanotori. These forces include vdW force, centrifugal force and the force of gravity. It should be mentioned that the effect of frictional forces, because of being insignificant with respect to other acting forces, are neglected in this work [10]. The vdW force is modeled by LJ potential as given in Eq. (4). The centrifugal and gravitational forces and their corresponding potential energies are respectively defined by Eq. (5a) and Eq. (5b) as

$$F_c = -mR\omega^2, \qquad E_c = -\frac{mR^2\omega^2}{2} \tag{5a}$$

$$F_g = -mg, \qquad E_g = -mgh \tag{5b}$$

In the above expressions, m is the mass of nanosector, R is the distance between the rotating body and origin, ω is the constant angular velocity, g is the acceleration of gravity and h is the vertical distance from an arbitrary base level. Thus, the total potential energy can be calculated from $E^{tot} = E_c + E_g + E_{vdW}$. The preferred position of the orbiting nanosector is the location of the minimum total potential energy. Based on the Newton's second law and assuming that the center of nanosector is defined by (R, Θ, Z) in the cylindrical coordinate system, one can arrive at [38]

$$m\left(\ddot{R} - R\dot{\Theta}^2\right) = -\frac{\partial E_{vdW}}{\partial R}, \quad m\left(R\ddot{\Theta} + 2\dot{R}\dot{\Theta}\right) = -\frac{1}{R}\frac{\partial E_{vdW}}{\partial \Theta}, \quad m\left(\ddot{Z} - g\right) = -\frac{\partial E_{vdW}}{\partial Z} \tag{6}$$

in which dot denotes the derivative with respect to time. Since, it is assumed that $R = c + \varepsilon\cos\varphi_1$ and $Z = \varepsilon\sin\varphi_1$ are fixed in the space and the nanosector orbits with a constant angular velocity around the z-axis, Eq. (6) can be simplified to

$$\frac{\partial E_{vdW}}{\partial R} = mR\omega^2, \quad \frac{\partial E_{vdW}}{\partial \Theta} = 0, \quad \frac{\partial E_{vdW}}{\partial Z} = mg \tag{7}$$

4. VdW potential energy and interaction force

In this section, using the continuum approximation, the formulations to estimate vdW interactions for an offset sector of nanotorus orbiting inside a nanotori molecule are given.

4. 1. Potential energy

The schematic of the nanosector orbiting inside an outer torus is shown in Fig. 1. From this figure, one can define a typical point on the nanotorus in the Cartesian coordinate system as

$$x_t = (c + b\cos\emptyset)\cos\theta\,, \; y_t = (c + b\cos\emptyset)\sin\theta, \qquad z_t = b\sin\emptyset \tag{8}$$

In addition, the location of a typical point on the nanosector is given by

$$x_s = (c + a\cos\varphi + \varepsilon\cos\varphi_1)\cos\Theta,$$

$$y_s = (c + a\cos\varphi + \varepsilon\cos\varphi_1)\sin\Theta,$$

$$z_s = a\sin\varphi + \varepsilon\sin\varphi_1 \tag{9}$$

in which ε is the distance between the central axes of nanosector and outer torus.

Since the gravitational force is negligible in comparison with vdW and centrifugal forces [38], the effect of this force is not incorporated into the calculations. As a result, one can deduce that φ_1 is equal to zero. Thus, the distance ρ between two typical element surfaces can be determined from

$$\rho^2 = (b-a)^2 + \varepsilon^2 + 2a\varepsilon - 2b\varepsilon + 4ab\sin^2\left(\frac{\phi-\varphi}{2}\right) + 4b\varepsilon\sin^2\left(\frac{\phi}{2}\right) - 4a\varepsilon\sin^2\left(\frac{\varphi}{2}\right) + 4(c + b\cos\phi)(c + a\cos\varphi + \varepsilon)\sin^2\left(\frac{\theta-\Theta}{2}\right) \tag{10}$$

So, the vdW potential energy can be written as

$$E_{vdW}(\varepsilon) = \eta_g^2 ab \int_0^{2\pi}\int_0^{2\pi}\int_0^{\beta}\int_0^{2\pi}\left(-\frac{A}{\rho^6} + \frac{B}{\rho^{12}}\right)(c + b\cos\phi)(c + a\cos\varphi + \varepsilon)\, d\theta\, d\Theta\, d\phi d\varphi \tag{11}$$

where η_g is the mean surface density of graphene.

Using analytical techniques in order to integrate Eq. (11) with respect to θ, the above quadruple integral reduces to a triple one as follows

$$E_{vdW}(\varepsilon) = \eta_g^2 ab \int_0^{2\pi}\int_0^{2\pi}\int_0^{\beta} G(\phi,\varphi)(c + b\cos\phi)(c + a\cos\varphi + \varepsilon)\, d\Theta\, d\phi d\varphi \tag{12}$$

where

$$G(\phi,\varphi) = \pi\sum_{k=1}^{2}\sum_{m=1}^{3k}\frac{H_k f_m^{(k)}}{P^{3k-m+\frac{1}{2}}(P+Q)^{m-\frac{1}{2}}} \tag{13}$$

Details for derivation of Eq. (13) are described in Appendix A.

Moreover, P and Q are defined by

$$P = (b-a)^2 + \varepsilon^2 + 2a\varepsilon - 2b\varepsilon + 4ab\sin^2\left(\frac{\phi-\varphi}{2}\right) + 4b\varepsilon\sin^2\left(\frac{\phi}{2}\right) - 4a\varepsilon\sin^2\left(\frac{\varphi}{2}\right) \tag{14a}$$

$$Q = 4(c + b\cos\phi)(c + a\cos\varphi + \varepsilon) \tag{14b}$$

and constants parameters of Eq. (13) are as

follows

$$\begin{cases} H_1 = -A/4, & H_2 = B/128, \\ f_1^{(1)} = 3, & f_2^{(1)} = 2, & f_3^{(1)} = 3, \\ f_1^{(2)} = 63, & f_2^{(2)} = 35, & f_3^{(2)} = 30, & f_4^{(2)} = 30 & f_5^{(2)} = 35, & f_6^{(2)} = 63 \dots \end{cases} \quad (14c)$$

By integrating Eq. (12) with respect to Θ, the vdW potential energy takes the following form

$$E_{vdW}(\varepsilon) = \eta_g^2 ab\beta \int_0^{2\pi}\int_0^{2\pi} G(\phi,\varphi)(c + b\cos\phi)(c + a\cos\varphi + \varepsilon)\, d\phi d\varphi \quad (15)$$

Eventually, the semi-analytic formulation obtained for the vdW potential energy between the two nanostructures can be numerically evaluated. The semi-analytical expression obtained herein is fast-computing and less complex in comparison with the Hypergeometric functions.

4.2. Interaction force

The vdW interaction force can be obtained by differentiating Eq. (15) with respect to R as

$$F_{vdW}(\varepsilon) = \frac{\partial E_{vdW}(\varepsilon)}{\partial R} = \frac{\partial E_{vdW}(\varepsilon)}{\partial \varepsilon} = \eta_g^2 ab\beta \int_0^{2\pi}\int_0^{2\pi} \left(\frac{\partial G(\phi,\varphi)}{\partial \varepsilon}\right)(c + b\cos\phi)(c + \varepsilon + a\cos\varphi) d\phi d\varphi \quad (16)$$

Using Eq. (13), one can have

$$\frac{\partial G(\phi,\varphi)}{\partial \varepsilon} = -\pi \sum_{k=1}^{2}\sum_{m=1}^{3k} H_k f_m^{(k)} \left(\frac{(3k-m+\frac{1}{2})\frac{\partial P}{\partial \varepsilon}}{P^{3k-m+\frac{3}{2}}(P+Q)^{m-1/2}} + \frac{(m-\frac{1}{2})\left(\frac{\partial P}{\partial \varepsilon}+\frac{\partial Q}{\partial \varepsilon}\right)}{P^{3k-m+\frac{1}{2}}(P+Q)^{m+\frac{1}{2}}} \right) \quad (17)$$

in which

$$\frac{\partial P}{\partial \varepsilon} = 2\varepsilon + 2a - 2b + 4b\sin^2\left(\frac{\phi}{2}\right) - 4a\sin^2\left(\frac{\varphi}{2}\right) \quad (18a)$$

$$\frac{\partial Q}{\partial \varepsilon} = 4(c + b\cos\phi) \quad (18b)$$

5. Oscillation frequency

Using Eqs. (7) and (16) and neglecting the effect of gravity, the angular velocity of motion can be written as

$$\omega = \sqrt{\frac{F_{vdW}(\varepsilon)}{m(c+\varepsilon)}} \quad (19)$$

The oscillation frequency is also obtained as

$$f = \frac{1}{2\pi}\sqrt{\frac{F_{vdW}(\varepsilon)}{m(c+\varepsilon)}} \quad (20)$$

and

$$m = 2\pi a m_0 \eta_g \beta (c + \varepsilon) \quad (21)$$

in which m_0 is the mass of a single carbon atom.

As seen from Eqs. (16) and (21), both vdW interaction force and mass of the rotating body are proportional to the angle of nanosector and thus the angular velocity is independent of this angle.

6. Result and discussion

The main results concerning the effects of geometrical parameters on the characteristics of the considered system and the method used are discussed in detail in the next two subsections. The system studied in the present work is assumed to be generated by bending elastically two single-walled carbon nanotubes (SWCNTs) in which one has a shorter length and the joint between two ends of the larger torus is considered seamless. According to this configuration, one can be assured that no repulsive forces exist between the nanosector and the nanotori. Therefore, the sector has been sucked into the torus just before the closure of the torus with a suction energy as same as double-walled carbon nanotubes (DWCNTs). The numerical values of the constants used in this study are tabulated in Table. 1.

Table. 1. Constants values used in the numerical evaluations [16]

Attractive constant for graphene-graphene	$A = 15.2\ (\text{eV} \times \text{Å}^6)$
Repulsive constant for graphene-graphene	$B = 240000\ (\text{eV} \times \text{Å}^{12})$
Atom density for a graphene	$\eta_g = 0.3812\ (\text{Å}^{-2})$
Mass of a single carbon atom	$m_0 = 12 \times 1.661 \times 10^{-27}(\text{kg})$
Radius of (16,16)	$b = 10.846\ (\text{Å})$
Radius of (20,20)	$b = 13.557\ (\text{Å})$

6.1. Onset configuration

In this subsection, it is assumed that the nanosector and nanotori always remain concentric. For the given values of c, a and β, the tube radius of nanotori is determined to minimize the vdW potential energy. Thus, in this geometry, the orbiting body oscillates stably inside the nanotori.

The effect of changing the sector angle on the distribution of vdW potential energy is illustrated in Fig. 2.

According to this figure, as the sector angle gets larger the magnitude of minimum potential energy increases, while the value of the corresponding nanotorus tube radius remains unchanged. Moreover, this specific value of nanotorus tube radius is calculated in Table. 2. As seen, the difference between the tube radii of outer and inner nanotorus is calculated around 3.4 Å which corresponds to the radius difference of inner and outer tubes of MWCNT oscillators [11]. Moreover, to obtain the oscillation frequency of system, the centrifugal energy is equated with the maximum suction energy of DWCNTs as exposed in Ref. [40]. It must be noted that in this study the maximum suction energy is calculated based on Eq. (30) given by Ansari and Motevalli [18]. Since both centrifugal energy and maximum suction energy are proportional to the mass of sector or angle of sector, the present oscillation frequency is found to be independent of the sector angle as demonstrated in Table. 2.

The obtained results are also in good agreement with previous reports given by Hilder and Hill [40]. However, their oscillation frequency was found to be slightly affected by the sector angle.

6.2. Offset configuration

In this subsection, it is assumed that the cross-sectional center of the nanosector is located at a distance ε from the cross-sectional center of the nanotorus. In this case, the equilibrium position of system is determined for different geometries. Moreover, the effects of geometrical parameters such as ring radius, tube radius of nanotorus and sector angle on the equilibrium position, distributions of vdW interactions and oscillation frequency are examined.

In Fig. 3, for two values of nanotorus tube radius, the distribution of vdW potential energy and interaction force are displayed against the offset position of nanosector.

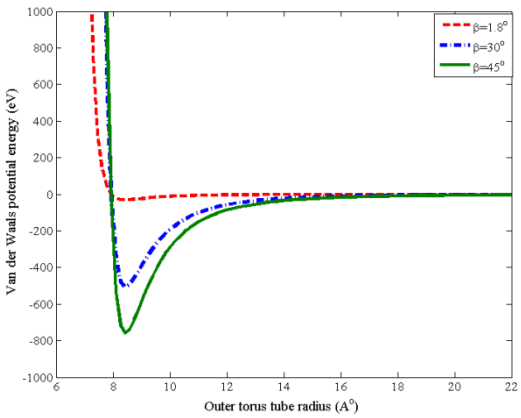

Fig. 2. Distribution of vdW potential energy for concentric configuration versus outer torus radius for various angles of sector ($c = 1500\ Å$, $a = 5\ Å$)

Table. 2. Comparison of the obtained oscillation frequencies with the ones given in Ref. [40]

a (Å)*	c (Å)*	β (degree)*	b (Å) Present study	b (Å) Ref. [40]	Frequency (GHz) Present study	Frequency (GHz) Ref. [40]
5	1500	1.8	8.49	8.45	0.984	0.962
5	1500	30	8.49	8.45	0.984	0.984
5	1500	45	8.49	8.45	0.984	0.984
6.5	110	45	9.796	9.97	13.027	12.9
6.78	200	45	10.29	10.225	7.145	7.09
7	150	45	10.45	10.431	9.4836	9.41

* Taken from [40]

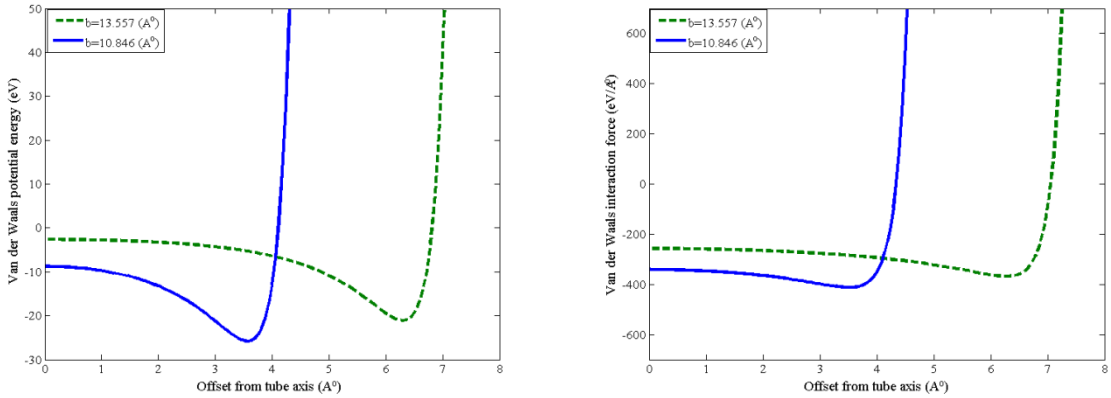

(a) **(b)**

Fig. 3. Distribution of **(a)** potential energy **(b)** vdW interaction force versus offset position for different tube radii ($\beta = 4.6^0, c = 1500\ \mathring{A}\ , a = 4.071\ \mathring{A}$)

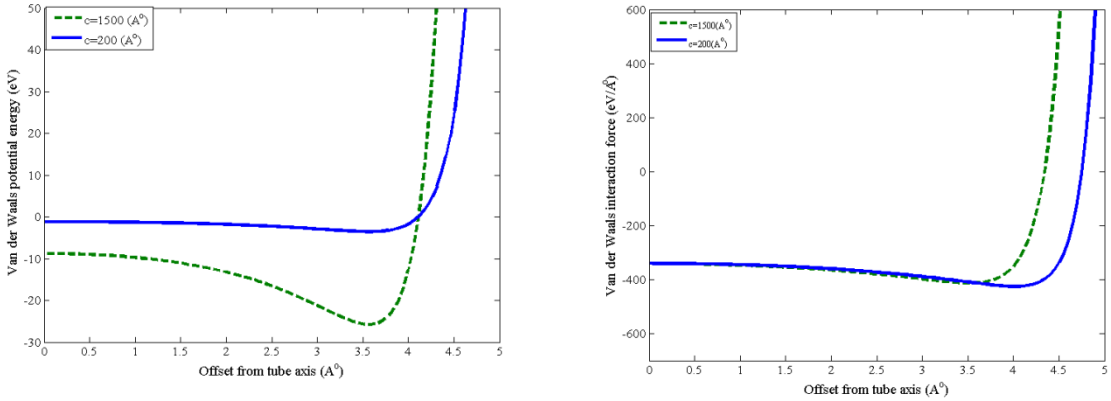

(a) **(b)**

Fig. 4. Distribution of **(a)** potential energy **(b)** vdW interaction force versus offset position for various ring radii ($\beta = 4.6^0, b = 10.846\ \mathring{A}\ , a = 4.071\ \mathring{A}$)

In order to clarify the veracity of the present result, the vdW potential energy for the offset sector is compared with that reported by Baowan et al. [16] for an offset SWCNT inside a SWCNT of larger radius. To accomplish this, the ring radius is taken to be 1500 Å and the sector angle is obtained as 4.6^0. In this case, the nanotori and the sector inside correspond well to a MWCNT. As can be seen, for a torus created by joining the two ends of a (16,16) CNT and a sector with the tube radius of 4.071 Å, the minimum potential energy occurs where the amount of offset is 3.515 Å. This amount changes to 6.303 Å when a (20,20) tube is used as the outer torus. These values indicate that the sector tends to get closer to the wall of the nanotorus as the nanotori tube radius gets larger. It should be mentioned that the interspacing magnitude between the walls of the inner and the outer tube for a stable system is always ~3.4Å. The effect of changing the tube radius of the nanotorus on the distribution of vdW interaction force is also similar to the vdW potential energy alteration. The variations of vdW potential energy and interaction force with respect to offset position of sector are depicted in Fig. 4 for two values of ring radius. In conformity with this figure, one can deduce that the value of minimum potential energy increases by increasing the value of ring radius, while the equilibrium position remains unaltered.

The graphs of vdW interaction force in contrast have a smooth alternation till around $\varepsilon = 3.5$ Å as shown in the figure. However, after this point, the magnitude of vdW interaction force considerably increases as the ring radius becomes larger. It is also worth mentioning that changing the ring radius changes the position of minimum vdW interaction force.

The influence of changing the sector angle on the vdW interactions is shown in Fig. 5.

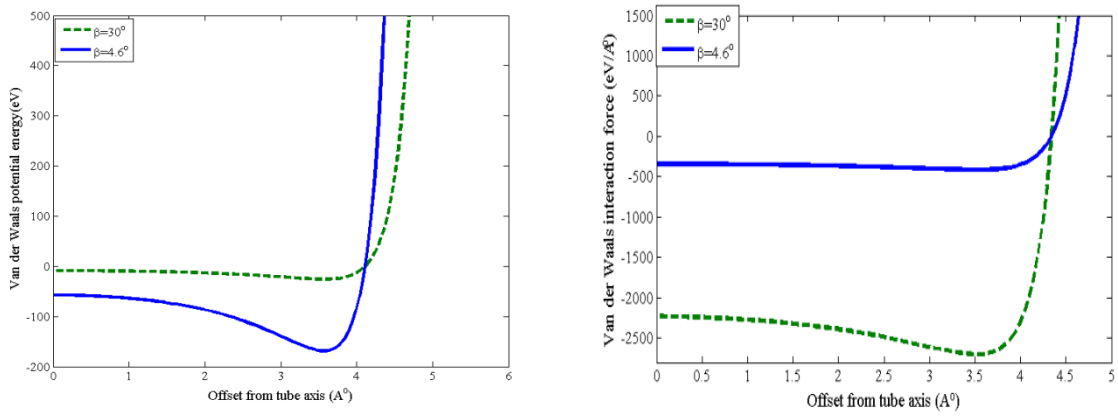

(a) **(b)**

Fig.5 Distribution of **(a)** potentialenergy **(b)** vdW interaction forceversus offset position for various angles of sector($c = 1500\ Å\ , b = 10.846\ Å\ , a = 4.071\ Å$)

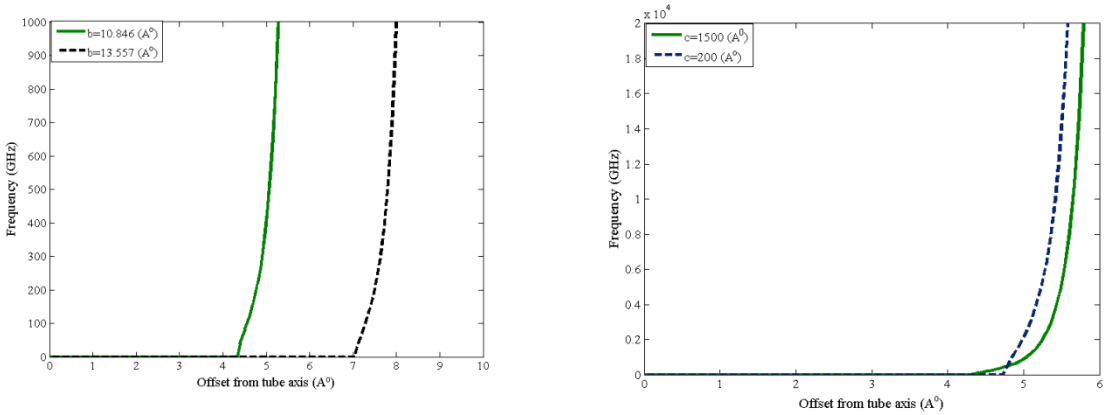

(a) **(b)**

Fig. 6. Effect of **(a)** tube radius $(c = 1500\ Å)$ **(b)** ring radius $(b = 10.846\ Å)$on the frequency against offset position ($\beta = 4.6^0, a = 4.071\ Å$)

Likewise Fig. 2, changing the sector angle only affects the magnitude of minimum potential energy and interaction force so that the equilibrium position is completely independent of this angle.

Finally, for different geometrical parameters, frequency versus offset position of nanosector is depicted in Fig. 6.

As mentioned in Section 5, the oscillation frequency does not depend on the angle of the sector. Therefore, only the effects of nanotorus tube radius and ring radius on the frequency characteristics have been investigated. According to this figure, there is no oscillation frequency until near the equilibrium position of the system. In other words, the system starts to oscillate after the vdW interaction force experiences its positive values. However, after this point the magnitude of frequency which is in the GHz range considerably increases. Finally, it is found that smaller values of ring radius provide larger oscillation frequencies for a given value of offset position.

7. Conclusion

Using the continuum approximation along with the 6-12 LJ potential function, the mechanics of a nanosector orbiting inside a nanotori molecule was studied. To this end, a semi-analytical formulation was obtained in terms of double integrals which enables one to readily calculate the vdW potential energy and interaction force between the interacting entities. Afterwards, based on the Newton's second law and ignoring the effects of gravitational and frictional forces, a new expression was presented to evaluate the oscillation frequency. The perfect position of nanosector inside carbon nanotorus was examined. The effects of geometrical parameters on the distributions of vdW interactions as well as the corresponding equilibrium position and oscillation frequency

were investigated. It was found that the equilibrium position tends to get closer to the wall of the outer tube as the outer torus radius increases, whereas this position remains unchanged as the sector angle or the ring radius changes. Besides, it was concluded that the obtained oscillation frequency is independent of the sector angle.

References

[1] S. Iijima, 1991, Helical microtubules of graphitic carbon. Nature 354(6348), 56.

[2] J.R. Minkel, 2002, Focus: Nanotubes in the Fast Lane. Physics 9, pp. 4.

[3] M. Damnjanović, I. Milošević, T. Vuković, R. Sredanović, 1999, Full symmetry, optical activity, and potentials of single-wall and multiwall nanotubes. Physical Review B 60(4), pp. 2728.

[4] R.E. Tuzun, D.W. Noid, B.G. Sumpter, 1995, The dynamics of molecular bearings. Nanotechnology, 6(2), p. 64.

[5] B.J. Cox, N. Thamwattana, J.M, Hill, 2008, Mechanics of nanotubes oscillating in carbon nanotube bundles. In Proceedings of the Royal Society of London A: Mathematical, Physical and Engineering Sciences 464(2091), pp. 691-710.

[6] Z. Zhang, T. Li, 2011, Ultrafast nano-oscillators based on interlayer-bridged carbon nanoscrolls. Nanoscale Research Letters, 6(1), pp. 470.

[7] P. Liu, Y. Zhang, C. Lu, 2005, Oscillatory behavior of C_{60}-nanotube oscillators: a molecular-dynamics study. Journal of Applied Physics 97(9), 094313.

[8] J. Cumings, A. Zettl, 2000, Low-friction nanoscale linear bearing realized from multiwall carbon nanotubes. Science 289(5479), pp. 602-604.

[9] Q. Zheng, Q. Jiang, 2002, Multiwalled carbon nanotubes as gigahertz oscillators. Physical Review Letters 88(4), 045503.

[10] Q. Zheng, J.Z. Liu, Q. Jiang, 2002, Excess van der Waals interaction energy of a multiwalled carbon nanotube with an extruded core and the induced core oscillation. Physical Review B 65(24), 245409.

[11] S.B. Legoas, V.R. Coluci, S.F. Braga, P.Z. Coura, S.O. Dantas, D.S. Galvao, 2003, Molecular-dynamics simulations of carbon nanotubes as gigahertz oscillators. Physical Review Letters 90(5), 055504.

[12] S.B. Legoas, V.R. Coluci, S.F. Braga, P.Z. Coura, S.O. Dantas, D.S. Galvao, 2004, Gigahertz nanomechanical oscillators based on carbon nanotubes. Nanotechnology 15(4), S184.

[13] L.A. Girifalco, 1992, Molecular properties of fullerene in the gas and solid phases. The Journal of Physical Chemistry 96(2), pp. 858-861.

[14] L.A. Girifalco, M. Hodak, R.S. Lee, 2000, Carbon nanotubes, buckyballs, ropes, and a universal graphitic potential. Physical Review B 62(19), 13104.

[15] L. Henrard, E. Hernandez, P. Bernier, A. Rubio, 1999, van der Waals interaction in nanotube bundles: consequences on vibrational modes. Physical Review B 60(12), R8521.

[16] D. Baowan, N. Thamwattana, J.M. Hill, 2008, Suction energy and offset configuration for double-walled carbon nanotubes. Communications in Nonlinear Science and Numerical Simulation 13(7), pp. 1431-1447.

[17] M. Hodak, L.A. Girifalco, 2001, Fullerenes inside carbon nanotubes and multi-walled carbon nanotubes: optimum and maximum sizes. Chemical Physics Letters 350(5-6), pp. 405-411.

[18] R. Ansari, B. Motevalli, 2009, The effects of geometrical parameters on force distributions and mechanics of carbon nanotubes: A critical study. Communications in Nonlinear Science and Numerical Simulation, 14(12), pp. 4246-4263.

[19] R. Ansari, B. Motevalli, 2011, On new aspects of nested carbon nanotubes as gigahertz oscillators. Journal of Vibration and Acoustics 133(5), 051003.

[20] R. Ansari, E. Mahmoudinezhad, A. Alipour, M. Hosseinzadeh, 2013, A comprehensive study on the encapsulation of methane in single-walled carbon nanotubes. Journal of Computational and Theoretical Nanoscience 10(9), pp. 2209-2215.

[21] R. Ansari, E. Mahmoudinezhad, A. Alipour, M. Hosseinzadeh, 2013, A comprehensive study on the encapsulation of methane in single-walled carbon nanotubes. Journal of Computational and Theoretical Nanoscience 10(9), pp. 2209-2215.

[22] R. Ansari, M. Daliri, M. Hosseinzadeh, 2013, On the van der Waals interaction of carbon nanotubes as electromechanical nanothermometers. Acta Mechanica Sinica 29(4), pp. 622-632.

[23] R. Ansari, F. Sadeghi, A. Alipour, 2013, Oscillation of C_{60} fullerene in carbon nanotube bundles. Journal of Vibration and Acoustics 135(5), 051009.

[24] B.I. Dunlap, 1992, Connecting carbon tubules. Physical Review B 46(3), 1933.

[25] J. Liu, H. Dai, J.H. Hafner, D.T. Colbert, R.E.C. Smalley, C. Dekker, SJ Tans, LJ Geerligs, A. Bezryadin, J. Wu, and G. Wegner Towards transport on single molecules: first results on nanofabrication and phthalocyanine polymers in Atomic and Molecular Wires, eds. C. Joachim

and S. Roth (Kluwer Acad. Publ., 1997), Nature, 385, pp. 780-781.

[26] L. Liu, C.S. Jayanthi, S.Y. Wu, 2001, Structural and electronic properties of a carbon nanotorus: effects of delocalized and localized deformations. Physical Review B 64(3), 033412.

[27] J. Yuhara, M. Schmid, P. Varga, 2003, Two-dimensional alloy of immiscible metals: Single and binary monolayer films of Pb and Sn on Rh (111). Physical Review B 67(19), 195407.

[28] D.J. Klein, W.A. Seitz, T.G. Schmalz, 1986, Icosahedral symmetry carbon cage molecules. Nature, 323(6090), 703.

[29] C.L. Nagy, K. Nagy, M.V. Diudea, 2009, Elongated tori from armchair DWNT. Journal of Mathematical Chemistry 45(2), pp. 452-459.

[30] S. Itoh, S. Ihara, J.I. Kitakami, 1993, Toroidal form of carbon C_{360}. Physical Review B 47(3), 1703.

[31] S. Ihara, S. Itoh, J.I. Kitakami, 1993, Helically coiled cage forms of graphitic carbon. Physical Review B 48(8), 5643.

[32] S. Itoh, S. Ihara, 1994, Isomers of the toroidal forms of graphitic carbon. Physical Review B 49(19), 13970.

[33] N. Chen, M.T. Lusk, A.C. van Duin, W.A. Goddard III, 2005, Mechanical properties of connected carbon nanorings via molecular dynamics simulation. Physical Review B 72(8), 085416.

[34] M.B. Nardelli, B.I. Yakobson, J. Bernholc, 1998, Mechanism of strain release in carbon nanotubes. Physical review B 57(8), R4277.

[35] D.A. Walters, L.M. Ericson, M.J. Casavant, J. Liu, D.T. Colbert, K.A. Smith, R.E. Smalley, 1999, Elastic strain of freely suspended single-wall carbon nanotube ropes. Applied Physics Letters 74(25), pp. 3803-3805.

[36] M.F. Lin, D.S. Chuu, 1998, Persistent currents in toroidal carbon nanotubes. Physical Review B 57(11), p. 6731.

[37] B. Sun, 2010, Deformation, vibration, buckling of continuum nanotorus. Journal of Nanomaterials 2010, p. 26.

[38] T.A. Hilder, J.M. Hill, 2007, Orbiting atoms and C_{60} fullerenes inside carbon nanotori. Journal of Applied Physics 101(6), 064319.

[39] T.A. Hilder, J.M. Hill, 2007, Oscillating carbon nanotori along carbon nanotubes. Physical Review B 75(12), 125415.

[40] T.A. Hilder, J.M. Hill, 2007. Orbiting nanosectors inside carbon nanotori. Micro & Nano Letters 2(3), pp. 50-53.

[41] H. Sabzyan, M. Kowsar, 2017, Molecular dynamics simulations of electric field induced water flow inside a carbon nanotorus: a molecular cyclotron. Physical Chemistry Chemical Physics 19(19), pp. 12384-12393.

[42] H. Sabzyan, M. Kowsar, 2018, Molecular dynamics simulation of the cyclotron motion of ions in a carbon nanotorus induced by gigahertz rotating electric field. Molecular Simulation 44(4), pp. 263-273.

[43] C. Chuang, J. Guan, D. Witalka, Z. Zhu, B.Y. Jin, D. Tománek, 2015, Relative stability and local curvature analysis in carbon nanotori. Physical Review B 91(16), 165433.

[44] R.K. Lee, J.M. Hill, 2015, Design of a nanotori-metallofullerene logic gate. The ANZIAM Journal, 57(1), pp. 29-42.

[45] O.E. Glukhova, V.A. Kondrashov, V.K. Nevolin, I.I. Bobrinetsky, G.V. Savostyanov, M.M. Slepchenkov, 2016, Prediction of the stability and electronic properties of carbon nanotori synthesized by a high-voltage pulsed discharge in ethanol vapor. Semiconductors 50(4), pp. 502-507.

[46] M.R. Farahani, W. Gao, 2016, On multiplicative and redefined version of Zagreb indices of V-phenylenic nanotubes and nanotorus. British Journal of Mathematics & Computer Science 13(5), pp. 1-8.

[47] M.L. Loyola, M.L.A.N. De Las Peñas, G.M. Estrada, E.B. Santoso, 2015, Symmetry groups associated with tilings on a flat torus. Acta Crystallographica Section A: Foundations and Advances 71(1), pp. 99-110.

Appendix A

Here, the details of derivation of Eq. (13) are presented. To obtain this equation, integrals of the following forms must be calculated

$$I_n = \int_0^{2\pi} \frac{d\theta}{\rho^n} \quad ; \; n = 6,12 \tag{A1}$$

in which

$$\rho = \sqrt{P + Q\sin^2\left(\frac{\theta-\Theta}{2}\right)} \tag{A2}$$

and P and Q are defined by Eq. (14).

Substituting $x = \frac{\theta-\Theta}{2}$ and $m = \frac{n}{2}$ into Eq. (A.1) yields

$$I_m = 2\int_{-\frac{\Theta}{2}}^{\pi-\frac{\Theta}{2}} \frac{dx}{(P+Q\sin^2 x)^m} \tag{A3}$$

As shown in Ref. [40], the starting angle of the above equation is arbitrary, so Θ is taken to be zero. Thus, Eq. (A.3) is rewritten as

$$I_m = 2\int_0^{\pi} \frac{dx}{(P+Q\sin^2 x)^m} = 2\int_0^{\frac{\pi}{2}} \frac{dx}{(P+Q\sin^2 x)^m} + 2\int_{\frac{\pi}{2}}^{\pi} \frac{dx}{(P+Q\sin^2 x)^m} \tag{A4}$$

Substituting $y = \pi - x$ into Eq. (A4) for the interval $[\pi/2, \pi]$, one can arrive at

$$I_m = 4\int_0^{\pi/2} \frac{dx}{(P+Q\sin^2 x)^m} \quad \text{(A5)}$$

Letting $t = \cot x$ leads to

$$I_m = \frac{4}{P^m}\int_0^{\infty} \frac{(1+t^2)^{m-1}}{(t^2+\gamma^2)^m}\, dt \quad \text{(A6)}$$

in which $\gamma = \sqrt{\left(1+\frac{Q}{P}\right)}$

Using the substitution $t = \gamma\tan\psi$, the above formulation can be written as the form below

$$I_m = \frac{4}{P^m \gamma^{2m-1}}\int_0^{\pi/2} (1+\gamma^2\tan^2\psi)^{m-1}\,(\cos\psi)^{2m-2} d\psi \quad \text{(A7)}$$

Using Newton's binomial expansion, the above equation can be expressed as

$$I_m = \frac{4}{P^m}\sum_{k=0}^{m-1}\int_0^{\pi/2}\binom{m-1}{k}\frac{(\sin\psi)^{2m-2k-2}(\cos\psi)^{2k}}{\gamma^{2k+1}} d\psi \quad \text{(A8)}$$

Finally, after performing the prior equation analytically, the following form is obtained for Eq. (13)

$$G(\phi,\varphi) = -AI_3 + BI_6 = \pi\sum_{k=1}^{2}\sum_{m=1}^{3k}\frac{H_k f_m^{(k)}}{P^{3k-m+\frac{1}{2}}(P+Q)^{m-\frac{1}{2}}} \quad \text{(A9)}$$